Ultrashort broadband polarization beam splitter based on an asymmetrical directional coupler

Daoxin Dai,[1,2,*] Zhi Wang,[1] and John E. Bowers[1]

[1]*University of California Santa Barbara, ECE Department, Santa Barbara, California 93106, USA*

[2]*Centre for Optical and Electromagnetic Research, Zhejiang University, Zijingang Hangzhou 310058, China*

**Corresponding author: dxdai@ece.ucsb.edu*

Received May 16, 2011; revised June 7, 2011; accepted June 7, 2011;
posted June 8, 2011 (Doc. ID 147522); published July 1, 2011

An ultrashort polarization beam splitter (PBS) based on an asymmetrical directional coupler is proposed by utilizing the evanescent coupling between a strip-nanowire and a nanoslot waveguide. In order to be convenient for integration with other components, mode converters between the nanoslot waveguide and the strip-nanowire are introduced and merged into S-bends to achieve an ultracompact PBS. As an example a 6.9 μm long PBS based on a silicon-on-insulator platform is designed, and the length of the coupling region is as small as 1.3 μm. Numerical simulations show that the present PBS has a very broad band (>160 nm) for an extinction ratio of >10 dB. © 2011 Optical Society of America

OCIS codes: 130.2790, 230.7390, 230.5440.

A polarization beam splitter (PBS) is a basic functional element for many applications [1]. A short PBS is especially desired for on-chip networks. Waveguide-type PBSs have been reported using various structures, e.g, multimode interference (MMI) structures [2–6], directional couplers (DCs) [7–12], Mach–Zehnder interferometers (MZIs) [13–15], and photonic-crystal (PhC)/grating structures [16–18]. Figure 1 shows a summary for the sizes of the PBSs reported. The length of an MMI-based PBS is usually quite long [2–4] and could be shortened by using a quasi-state imaging effect [2] or by cascading structures [3]. However, it is still quite long (~1805 μm [2], ~10^4 μm [3]). MZI structures have also been used very widely for realizing PBSs [14]. In order to make a compact MZI PBS, a large birefringence is needed, e.g., by introducing additional stresses [19] or by using some highly birefringent materials, such as $LiNbO_3$ [20], III–V semiconductor compounds [21], and liquid crystals [22]. However, such PBSs are still relatively long (e.g., ~3300 μm [13], >10^4 μm [14], ~600 μm [15]). Another possible way to make a short PBS is by utilizing the strong polarization dependence of PhC structures (e.g., ~50 μm [16], ~20 μm [17]) or out-of-plane gratings (e.g., ~14 μm [18]). However, the design is usually quite complex, and the fabrication is relatively difficult. More importantly, the PhC structure usually introduces a relatively large loss.

The DC is a popular structure for PBSs because of its simplicity and easy design. However, the DC PBS is usually very long (e.g., ~1600 μm [11]) when one uses low index contrast (Δ) waveguides due to the weak birefringence. It is well known that Si nanowires [23] and nanoslot waveguides [24] provide a huge birefringence, which is attractive for realizing small PBSs [5,6,9,12,25,26]. In [25], the reported Si-nanowire-based PBS is as small as $7 \times 16\,\mu m^2$ by utilizing the huge polarization dependence of the coupling length. However, the slight evanescent coupling for TE polarization prevents it from achieving a high extinction ratio. In [26], the author presented a PBS with a 16 μm long coupling region, including two parallel Si nanowires, between which there was a nanoslot waveguide. However, in [26], the authors mentioned that the gap between waveguides can not be smaller than 230 nm, and thus the PBS length cannot be reduced further. Also, the design in [26] is like a parallelly cascaded coupling system, and thus the bandwidth is naturally smaller than a one-stage coupling system.

In this Letter, we utilize the evanescent coupling between a Si nanowire and a nanoslot waveguide and propose an ultrashort broadband PBS based on an asymmetrical DC structure, which is a one-stage coupling system. The gap between waveguides could be very small, which helps to obtain a PBS much shorter than that in [26]. In our design, mode converters between the nanoslot waveguide and the strip-nanowire are merged into S-bends, which is also helpful for achieving an ultracompact PBS. Figure 2 shows the three-dimensional view for the proposed ultrashort PBS. The cross section in the coupling region is also shown. We connect S-bends at both ends of the coupling region to make the two waveguides close or separated. In order to make them more convenient to integrate with other components in the same chip, we merge mode converters into S-bends. The mode converter between the nanoslot waveguide and the strip-nanowire is similar to that in [27]. In the coupling region, these two waveguides are designed to satisfy

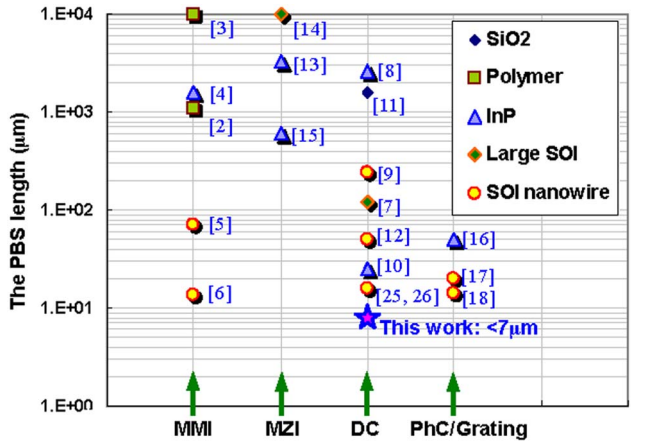

Fig. 1. (Color online) Summary of the dimensions of the PBSs reported (including the S-bend part if applied).

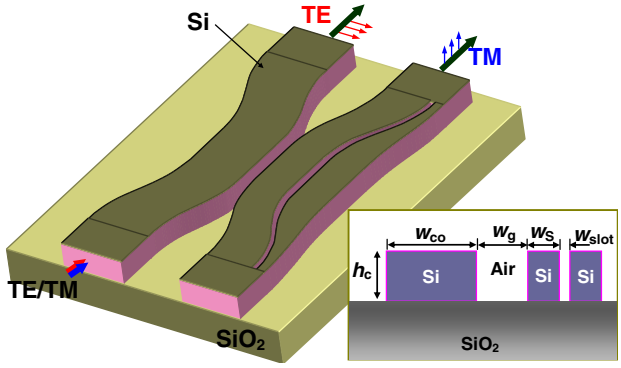

Fig. 2. (Color online) Schematic configuration of the proposed PBS.

the phase-matching condition for TM polarization, so that it could be coupled to the cross port completely when the length of the coupling region is chosen appropriately. On the other hand, for TE polarization, a nanoslot waveguide usually has a much lower effective index than a strip-nanowire, so TE-polarized light will not satisfy the phase-matching condition for the evanescent coupling. Thus, TE-polarized light goes through the strip-nanowire almost without coupling. In this way, TE- and TM-polarized light are separated within a very short length, which is close to the coupling length of TM polarization.

In this Letter, we use a silicon-on-insulator (SOI) wafer with $H = 250\,\text{nm}$. The refractive indices of Si and SiO_2 are $n_{Si} = 3.455$ and $n_{SiO_2} = 1.445$, and that of air is $n_{air} = 1.0$. Air cladding is considered because it might be not very easy to fill the nanoslots with SiO_2. A finite element method (FEM) mode solver (from COMSOL) is used. Figure 3 shows the calculated effective indices of a strip-nanowire and a nanoslot waveguide. In our calculations, the nanoslot width is chosen as $w_{slot} = 60$, 80, and 100 nm. From Fig. 3, for TM polarization, the effective indices of the two different types of waveguides are quite close, and consequently one could satisfy the phase-matching condition (i.e., $n_{TM1} = n_{TM2}$) by choosing the core width w_{co} and w_{Si} appropriately. For example, when choosing $w_{co} = 0.4\,\mu\text{m}$ for the strip-nanowire, one has an optimal width $w_{Siopt} = 0.26\,\mu\text{m}$ for the nanoslot waveguide with $w_{slot} = 60\,\text{nm}$. The TM polarization modes for these two waveguides have the same effective index ($n_{TM1} = n_{TM2} = 1.68967$). Therefore, TM-polarized light will be coupled to the cross port completely when the length of the coupling region is

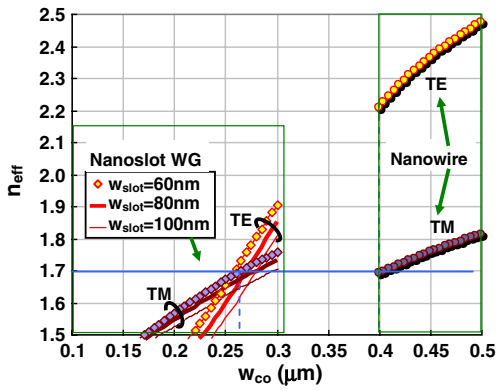

Fig. 3. (Color online) Effective indices of a Si nanowire and a nanoslot waveguide.

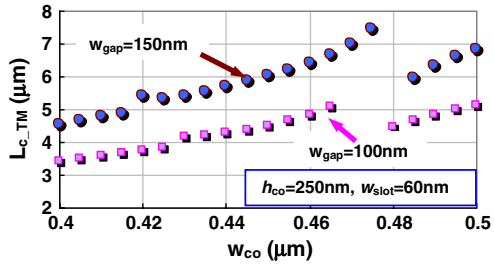

Fig. 4. (Color online) Coupling length for TM polarization.

chosen appropriately. On the other hand, when one chooses $w_{Si} = w_{Siopt}$, the two optical waveguides have very different effective indices for TE polarization, as shown by the circles in Fig. 3. The huge difference $(n_{eff1} - n_{eff2})_{TE}$ indicates that there is a serious phase mismatching, and consequently the evanescent coupling is depressed very significantly for TE-polarized light.

Figure 4 shows the coupling length calculated by $L_c = \pi/(\beta_{1TM} - \beta_{2TM})$, where β_{1TM} and β_{2TM} are the propagation constants for the first and second order supermodes for TM polarization. From this figure, it can be seen that a shorter coupling length is achieved by reducing the gap width. For the case of $w_{gap} = 100\,\text{nm}$, when choosing $w_{co} = 0.4\,\mu\text{m}$, the coupling is as short as $3.4\,\mu\text{m}$, which helps in obtaining an ultrasmall PBS. Figures 5(a) and 5(b) show the light propagation for TE and TM polarizations in the designed DC PBS. For the S-bends here, we choose the bending radius $R = 10\,\mu\text{m}$ and $\theta = 8°$, so that the bending loss is negligible and the end separation S is large enough to avoid any undesired coupling. Because of the coupling in the S-bend part, the optimal length of the coupling region is $1.3\,\mu\text{m}$, which is shorter than the coupling length ($\sim 3.4\,\mu\text{m}$) shown in Fig. 4. As shown in Figs. 5(a) and 5(b), we merge mode converters into the S-bends at the side of the nanoslot waveguide in order to minimize the footprint. In the section of the mode converter, one Si core of the nanoslot waveguide is tapered to be as narrow as 60 nm (considering the limitation of the fabrication technology), while the other Si core is tapered to match a strip-nanowire. There is some reflection at the junction, and fortunately it is very small, because the field amplitude at the slot is small for the coupled TM polarization.

Figure 6(a) shows the calculated transmission spectral responses at the through and cross ports for TE and TM

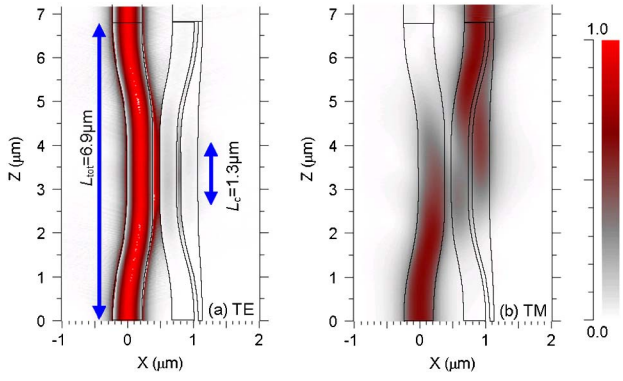

Fig. 5. (Color online) Light propagation in the designed PBS with $w_{co} = 0.4\,\mu\text{m}$, $w_{Si} = 0.26\,\mu\text{m}$, $h_{co} = 250\,\text{nm}$, $w_{slot} = 60\,\text{nm}$, and $w_{gap} = 100\,\text{nm}$. (a) TE, (b) TM.

polarizations, respectively. Since there is almost no coupling for TE polarization due to the phase mismatching, the response for TE polarization is very broadband. For extinction ratios of 10 dB and 20 dB, the bandwidth is about 160 nm and 60 nm, respectively. The extinction ratio is defined as the ratio between the powers of two polarizations at the same port. Usually a DC is sensitive to the dimension deviation due to the fabrication errors. The etching depth might be nonuniform due to the lag effect. For the present design, the negative influence of this effect could be minimized by introducing an overetching for the Si layer. In this way, it becomes tolerant to the etching depth. Therefore, we give an analysis for the case in which there is a waveguide width variation Δw, i.e., $w_{co} = w_{co} + \Delta w$, $w_{Si} = w_{Si} + \Delta w$, $w_{gap} = w_{gap} - \Delta w$, $w_{slot} = w_{slot} - \Delta w$. Figure 6(b) shows the transmission (at 1550 nm). It can be seen that one can still obtain a low loss as well as a good extinction ratio (>10 dB) even with the fabrication error of $-40\,\text{nm} < \Delta w < 30\,\text{nm}$. When the deviation is too large, e.g., 40 nm, the gap width is only 60 nm, and some coupling occurs for TE polarization. This is why the extinction ratio degrades significantly when the deviation $\Delta w = 40\,\text{nm}$.

In summary, we have proposed an ultrashort PBS by utilizing an asymmetrical DC with a strip-nanowire and a nanoslot waveguide. TM polarization is coupled to the cross port when the length of the coupling region is chosen appropriately. Also, TE-polarized light goes through the strip-nanowire almost without coupling. In order to improve the convenience of integration with other components in the same chip, mode converters are merged into S-bends for the conversion between the nanoslot waveguide and the strip-nanowire. This helps to make the PBS footprint very compact. A 6.9 μm long PBS based on an SOI platform has been designed as an example, in which the length of the coupling region is only 1.3 μm. To the best of our knowledge, it is the shortest PBS reported to date. The numerical simulation shows that the present PBS has a very broad band (~160 nm) for an extinction ratio of >10 dB. It also shows that there is a relatively large fabrication tolerance (e.g., ±30 nm) for the waveguide width.

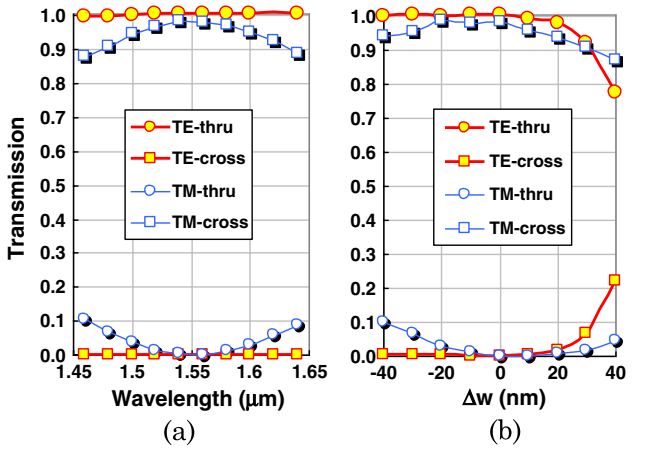

Fig. 6. (Color online) (a) Transmission spectral responses, (b) the transmissions (at 1550 nm) when there is a fabrication error Δw. The parameters are $w_{co} = 0.4\,\mu\text{m}$, $w_{gap} = 100\,\text{nm}$, $w_{slot} = 60\,\text{nm}$, $w_{Si} = 260\,\text{nm}$, and $L_c = 1.3\,\mu\text{m}$.

This work was supported by the Defense Advanced Research Projects Agency Microsystems Technology Office (DARPA MTO) under the Centers in Integrated Photonics Engineering Research (CIPhER) contract HR0011-10-1-0079.

References

1. T. Barwicz, M. Watts, M. Popovic, P. Rakich, L. Socci, F. Kartner, E. Ippen, and H. Smith, Nat. Photon. **1**, 57 (2007).
2. J. Hong, H. Ryu, S. Park, J. Jeong, S. Lee, E. Lee, S. Park, D. Woo, S. Kim, and B. H. O, IEEE Photon. Technol. Lett. **15**, 72 (2003).
3. Y. Jiao, D. Dai, Y. Shi, and S. He, IEEE Photon. Technol. Lett. **21**, 1538 (2009).
4. B. M. A. Rahman, N. Somasiri, C. Themistos, and K. T. V. Grattan, Appl. Phys. B **73**, 613 (2001).
5. A. Katigbak, J. Strother, and J. Lin, Opt. Eng. **48**, 080503 (2009).
6. B. K. Yang, S. Y. Shin, and D. M. Zhang, IEEE Photon. Technol. Lett. **21**, 432 (2009).
7. I. Kiyat, A. Aydinli, and N. Dagli, IEEE Photon. Technol. Lett. **17**, 100 (2005).
8. L. M. Augustin, J. J. G. M. van der Tol, R. Hanfoug R. W. J. M. de Laat, M. J. E. van de Moosdijk, P. W. L. van Dijk, Y.-S. Oei, and M. K. Smit, J. Lightwave Technol. **25**, 740 (2007).
9. J. Xiao, X. Liu, and X. Sun, Jpn. J. Appl. Phys. **47**, 3748 (2008).
10. X. G. Tu, S. S. N. Ang, A. B. Chew, J. H. Teng, and T. Mei, IEEE Photon. Technol. Lett. **22**, 1324 (2010).
11. T. Yamazaki, H. Aono, J. Yamauchi, and H. Nakano, J. Lightwave Technol. **26**, 3528 (2008).
12. Y. Yue, L. Zhang, J.-Y. Yang, R. G. Beausoleil, and A. E. Willner, Opt. Lett. **35**, 1364 (2010).
13. L. B. Soldano, A. H. de Vreede, M. K. Smit, B. H. Verbeek, E. G. Metaal, and F. H. Groen, IEEE Photon. Technol. Lett. **6**, 402 (1994).
14. T. K. Liang and H. K. Tsang, IEEE Photon. Technol. Lett. **17**, 393 (2005).
15. L. M. Augustin, R. Hanfoug, J. J. G. M. van der Tol, W. J. M. de Laat, and M. K. Smit, IEEE Photon. Technol. Lett. **19**, 1286 (2007).
16. Y. Shi, D. Dai, and S. He, IEEE Photon. Technol. Lett. **19**, 825 (2007).
17. X. Ao, L. Liu, W. Lech, and S. He, Appl. Phys. Lett. **89**, 171115 (2006).
18. J. Feng and Z. Zhou, Opt. Lett. **32**, 1662 (2007).
19. M. Rajarajan, C. Themistos, B. M. A. Rahman, and K. T. V. Grattan, J. Lightwave Technol. **15**, 2264 (1997).
20. P. Wei and W. Wang, IEEE Photon. Technol. Lett. **6**, 245 (1994).
21. F. Ghirardi, J. Brandon, M. Carre, A. Bruno, L. Meniganx, and A. Carenco, IEEE Photon. Technol. Lett. **5**, 1047 (1993).
22. Q. Wang, G. Farrell, and Y. Semenova, IEEE J. Sel. Top. Quantum Electron. **12**, 1349 (2006).
23. D. Dai, Y. Shi, and S. He, Appl. Opt. **45**, 4941 (2006).
24. V. R. Almeida, Qianfan Xu, C. A. Barrios, and M. Lipson, Opt. Lett. **29**, 1209 (2004).
25. H. Fukuda, K. Yamada, T. Tsuchizawa, T. Watanabe, H. Shinojima, and S. Itabashi, Opt. Express **14**, 12401 (2006).
26. M. Komatsu, K. Saitoh, and M. Koshiba, Opt. Express **17**, 19225 (2009).
27. N.-N. Feng, R. Sun, L. C. Kimerling, and J. Michel, Opt. Lett. **32**, 1250 (2007).